SUPPLEMENTARY FIGURES

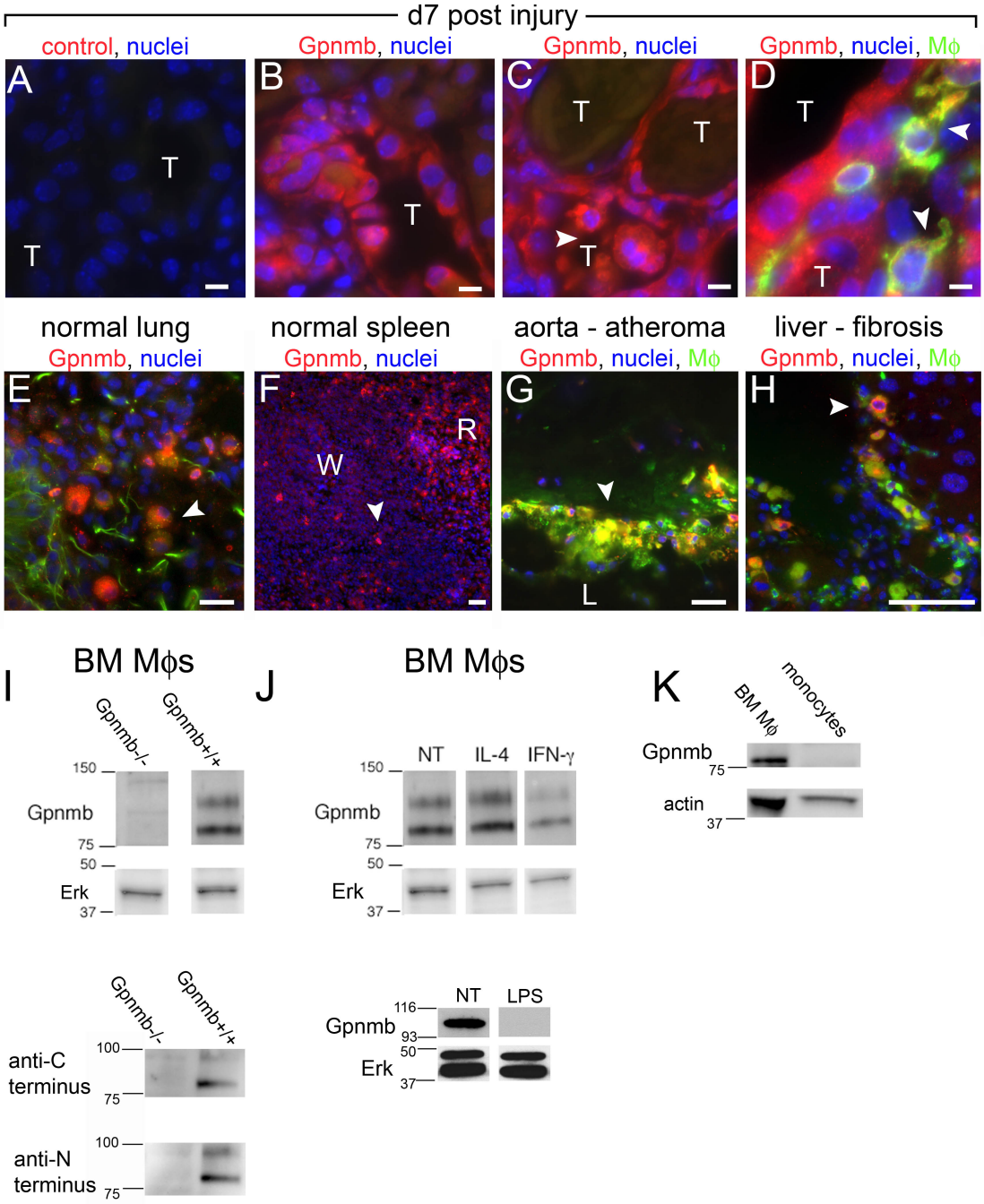

FIGURE S1. Pattern of Gpnmb expression in mouse kidney, other mouse tissues and macrophages. (***A-D***) Control antibody (***A***) or anti-N terminal Gpnmb detection in d7 post IRI kidney outer medulla (***B-C***) [T-tubule]. Note intratubular phagocytes [arrowhead].

Co-labeling for macrophages [arrowheads] (***D***) in inner medulla shows positivity in intracellular compartments. Anti-N terminal Gpnmb detection normal lung (***E***) showing positive staining in alveolar macrophages. (***F***) Low-power view of spleen showing high expression of Gpnmb in the red pulp [R], and only a few positive cells in white pulp [W], identified as tingible body macrophages (arrows). (***G***) Gpnmb (red) and CD68 (green) labeling of aortic arch atheromatous plaque from d165 ApoE-/- mice fed on high fat diet. The aortic lumen is denoted [L]. Gpnmb and CD68 co-localize in lesional macrophages. (***H***) Immunofluorescence for Gpnmb (red) and macrophage marker CD68 (green) in fibrotic scars in mouse livers after 12 weeks of CCl_4 injury. Note large round phagocytes (long arrow) co-express CD68 and Gpnmb whereas smaller CD68 +ve Mϕs (small arrow) and Kupffer cells (short arrow) lack Gpnmb. (***I***) Western blot of whole cell lysates from BMMϕs detecting Gpnmb using anti-C terminal antibodies (upper) or comparing both anti-N and anti-C termini antibodies (lower). (***J***) Detection of Gpnmb in unstimulated or 24h stimulated BMMϕs whole cell lysates. Note that both IFNγ and LPS down-regulate Gpnmb expression. (***K***) Detection of Gpnmb in blood monocytes compared with BMMϕs (bar $= 50\mu$m).

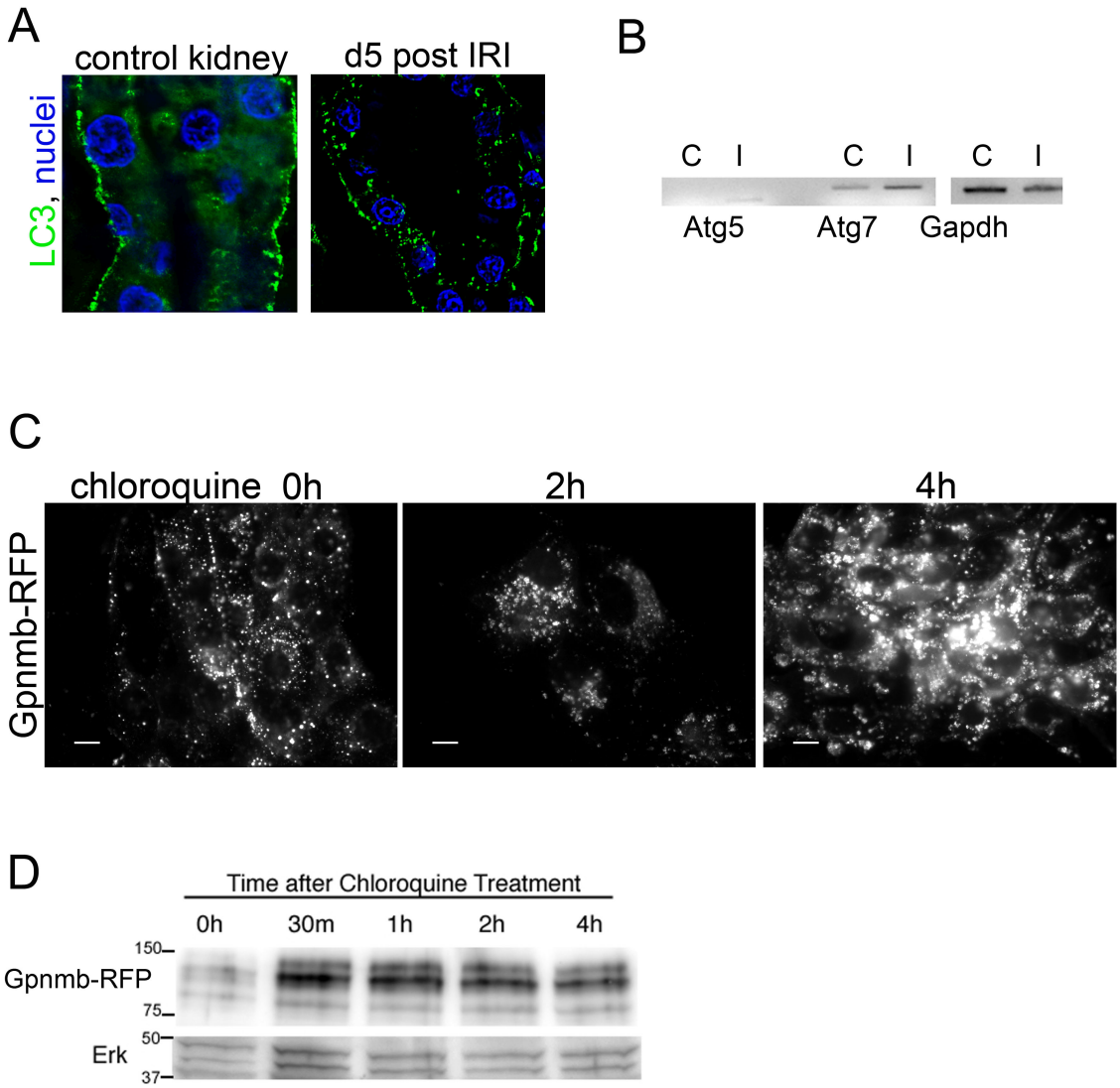

FIGURE S2. Characterization of autophagosomes in kidney tubule cells *in vivo* and *in vitro*. (***A***) Confocal images of antibody detected endogenous LC3 in normal proximal tubule of rat kidney and 5d post IRI. Note redistribution of LC3 in the injured tubules from a cytosolic and basement membrane distribution to an endosomal distribution. (***B***) RT-PCR for Atg protein transcripts from healthy proximal tubule cells purified from mouse kidney 'C' or injured proximal tubules purified from d5 post IRI kidney'I'. Note that both *Atg5* and *Atg7* are upregulated following injury. (***C***) Fluorescent micrographs of

Gpnmb-RFP+ expressing LLC-PK1 kidney epithelial cells at timepoints following chloroquine treatment. Note rapid accumulation and expansion of Gpnmb-RFP+ vesicles. (***D***) Immunoblot detecting Gpnmb-RFP in Gpnmb-RFP cells at timepoints after chloroquine treatment.

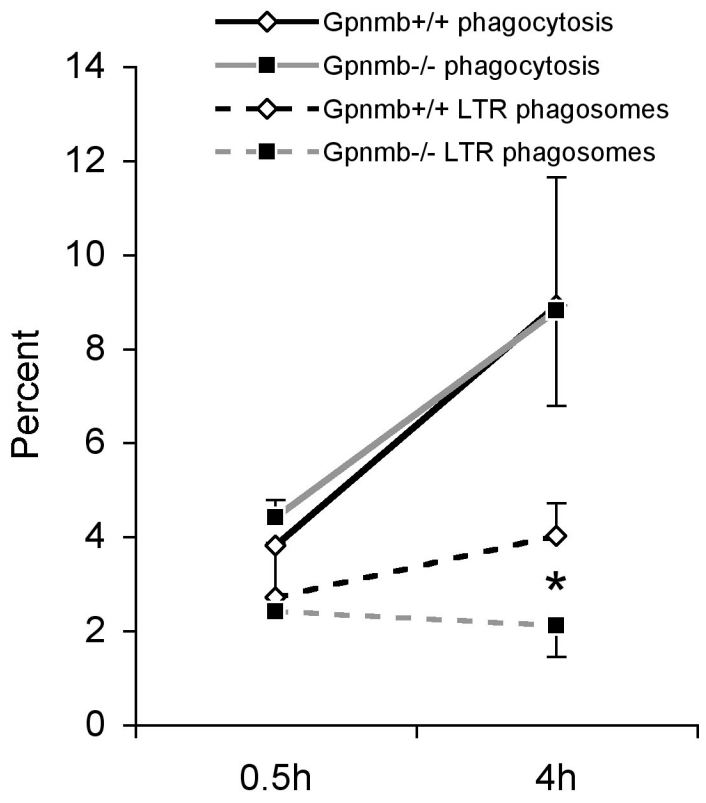

FIGURE S3. Acidification of apoptotic body containing phagosomes is delayed in *Gpnmb*$^{-/-}$ peritoneal macrophages *in vivo*. Graph showing the % phagocytosis by d4 thioglycollate peritoneal macrophages at 30min and 4h after IP injection of 10million apoptotic thymocytes (solid lines) and also the % of macrophages with lysotracker red +ve acidified phagosomes. Phagosomes in *Gpnmb*$^{+/+}$ macrophages were observed to undergo acidification while those of*Gpnmb*$^{-/-}$ macrophages did not (n=4/group * $P < 0.05$).

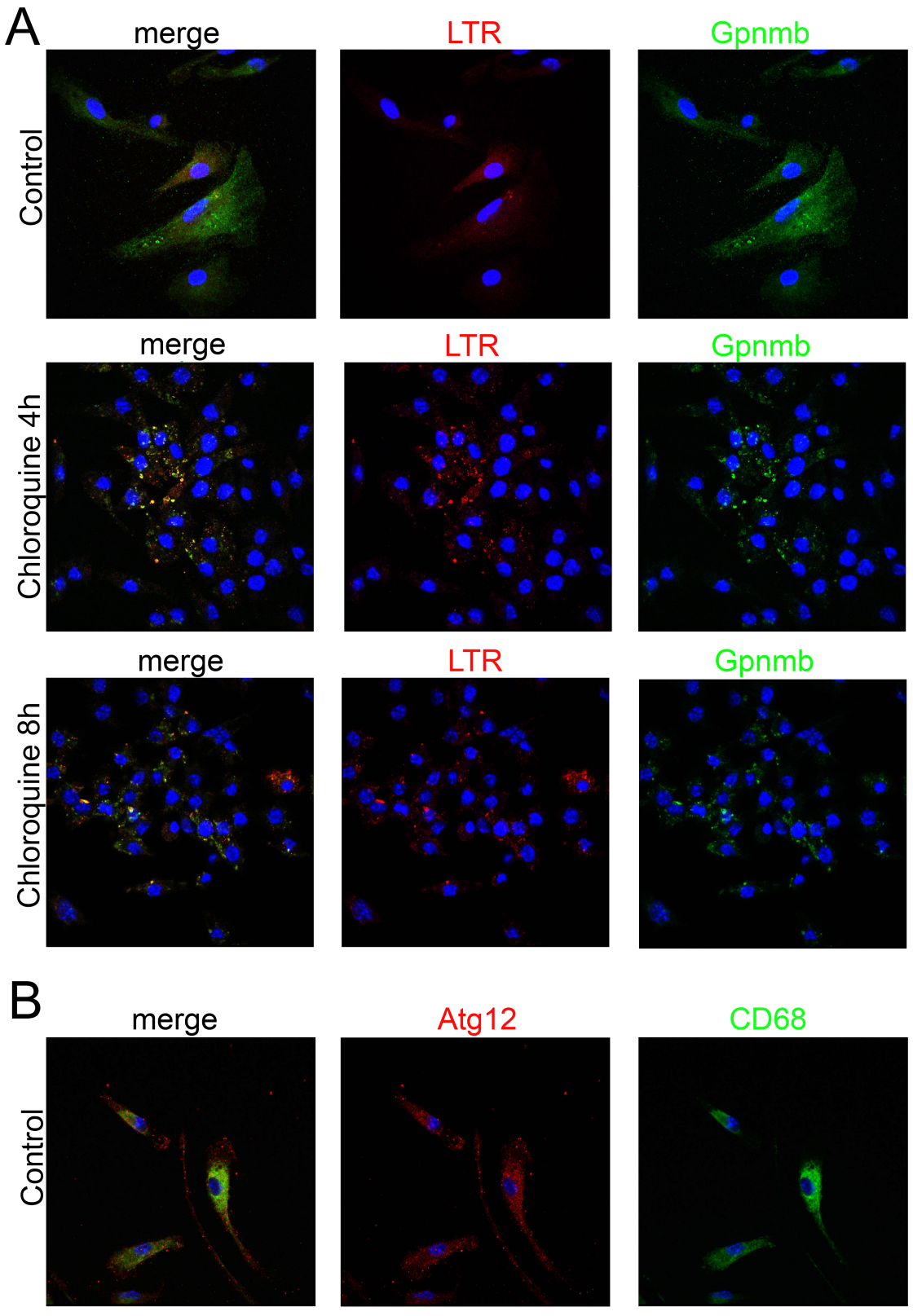
A
merge
LTR
Gpnmb
Control
merge
LTR
Gpnmb
Chloroquine 4h
merge
LTR
Gpnmb
Chloroquine 8h
B
merge
Atg12
CD68
Control

FIGURE S4. Characterization of Gpnmb compartments in macrophages. (***A***) Confocal images of Gpnmb (green) and lysotracker red in control or chloroquine treated BMMϕs. (***B***) Confocal images for Atg12 and CD68 in control BMMϕs